



Ordering-enhanced dislocation glide in III-V alloys

William E. McMahon, Joongoo Kang, Ryan M. France, Andrew G. Norman, Daniel J. Friedman, and Su-Huai Wei

Citation: *Journal of Applied Physics* **114**, 203506 (2013); doi: 10.1063/1.4833244

View online: <http://dx.doi.org/10.1063/1.4833244>

View Table of Contents: <http://scitation.aip.org/content/aip/journal/jap/114/20?ver=pdfcov>

Published by the [AIP Publishing](#)



Re-register for Table of Content Alerts

Create a profile.



Sign up today!



Ordering-enhanced dislocation glide in III-V alloys

William E. McMahon,^{a)} Joongoo Kang, Ryan M. France, Andrew G. Norman, Daniel J. Friedman, and Su-Huai Wei
 National Renewable Energy Laboratory, Golden, Colorado 80401, USA

(Received 6 September 2013; accepted 8 November 2013; published online 25 November 2013)

Ordering-induced effects on dislocations in metallic alloys have been extensively studied due to their importance in technology applications. We demonstrate that dislocation behavior in ordered III-V semiconductor alloys can be drastically different. This is because ordering in bulk metallic alloys is generally stable, whereas the surface-stabilized group-III sublattice ordering of a III-V alloy is only metastable in the bulk. Here, we show that dislocation glide can release some of the energy stored by ordering of III-V alloys, enhancing the glide of any dislocation which cuts through the ordered layers to create an antiphase boundary in the ordering pattern. This leads to an experimentally observed glide-plane switch which is unique to ordered III-V alloys. Implications for other unique strain-relaxation processes in III-V ordered alloys are also discussed. © 2013 AIP Publishing LLC. [<http://dx.doi.org/10.1063/1.4833244>]

I. INTRODUCTION

The movement of dislocations in a material in response to applied stresses can be greatly affected by the material's internal structure. Here, we will demonstrate that metastable group-III sublattice ordering can significantly alter the characteristics of dislocation glide in a III-V alloy, and offers a remarkable contrast to the more familiar behavior of dislocations in metal alloys. Sublattice ordering of III-V alloys can alter important material properties such as the band gap without changing either the alloy composition or the lattice constant.¹ Recent experimental results indicate that ordering can also affect dislocation motion;² here, we will examine the underlying energetics, in order to better understand and control strain relaxation during lattice-mismatched epitaxial growth.

Although structurally similar to stable ordered phases in metal alloys, CuPt-like ordered phases in III-V alloys are metastable,^{3,4} and therefore store energy which can subsequently be released by dislocation glide, if the dislocation creates an antiphase boundary (APB) as a result of its movement. In other words, the creation of an APB lowers the energy of the system, and consequently *increases* the glide force on the dislocation. This is in contrast to stable ordering in metal alloys, for which the creation of an APB by a dislocation raises the energy of the system and *decreases* the glide force on the dislocation.

If this were the only difference between the two cases (stable versus metastable ordering), then a simple change in the glide force would link the two cases. However, the situation is much more complicated. Dislocations in stable ordered metals generally travel in pairs. The first dislocation creates an APB, and the second one glides along the exact same plane in order to eliminate the APB and lower the energy. The distance between them is a balance between the APB energy (E_{APB}) and the interaction energy between the two dislocations.⁵ This pairing of dislocations fundamentally

alters many aspects of dislocation motion in ordered metal alloys, and, therefore, has been studied extensively.^{5,6}

For metastable ordering in III-V alloys, such pairings of dislocations are not expected nor observed. Instead, the APB created by a dislocation persists as a stable structure,^{7,8} and therefore the rules governing the motion of the associated dislocation will be quite different. The resulting APBs are also likely to alter the motion of subsequent dislocations and may impact the optoelectronic properties of subsequently grown materials and devices.⁹ Nonetheless, so far, very little is known about the effects of metastable ordering on dislocations in III-V alloys.

Experimentally, we have observed that group-III sublattice ordering can significantly alter the relaxation of lattice-mismatched III-V epilayers, and the threading dislocation density in subsequently grown devices. More interestingly, we observed an ordering-induced switch in the preference between two competing glide planes during the monolithic growth of multijunction photovoltaic devices with highly lattice-mismatched subcells.² Understanding and controlling strain relaxation mechanisms such as this is critical to developing lattice-mismatched solar cells with efficiencies above 45%,¹⁰ and other optoelectronic devices for which strain plays an important role.

In this paper, we first describe the geometry of a representative sample: compressively strained $\text{Ga}_x\text{In}_{1-x}\text{P}$ exhibiting CuPt-like ordering. Next, we determine the fundamental parameter characterizing APB formation in an ordered material—the APB energy—using *ab initio* structural calculations. The APB energy alters the glide force experienced by dislocations travelling through an ordered alloy and is therefore needed to accurately model every aspect of dislocation behavior. We then combine this result with an analytical force-equilibrium model to explain how ordering causes the preferred glide-plane to switch between two competing glide planes during the growth of strained $\text{Ga}_x\text{In}_{1-x}\text{P}$ epilayers. Finally, further implications and consequences are explored. Although this paper focuses on $\text{Ga}_x\text{In}_{1-x}\text{P}$ because it is extensively studied and well

^{a)}bill.mcmahon@nrel.gov

understood, the basic results can be extended to other ordered III-V alloys.

II. SAMPLE GEOMETRY

The sample configuration chosen for this study (Figure 1) consists of In-rich $\text{Ga}_x\text{In}_{1-x}\text{P}$ grown compressively strained on a GaAs (001) substrate miscut toward $(\bar{1}\bar{1}1)$ B. In this paper, the names “B+” and “B−” are linked to the asymmetry introduced by the sample miscut: a compressively strained epilayer rotates so as to have a higher average surface miscut angle for relaxation on the B+ plane, and a smaller average surface miscut angle for relaxation on the B− plane.¹¹ These rotations are a useful probe of relaxation, because the net epilayer “tilt” in x-ray diffraction (XRD) plots can be used to determine relative relaxation on the two planes.

Ordering introduces a second asymmetry. For the miscut direction shown, a single CuPt ordered variant is obtained in which adjacent B− planes alternate between being In-rich and Ga-rich. This ordering is stabilized near the growth surface by P-P dimers under certain conditions.¹² Once formed, it is metastable in the bulk and can be destroyed by annealing.¹³ As shown in Figure 1(b), dislocations which glide across the ordered planes can disrupt the ordering pattern. A dislocation gliding along a B+ plane creates an APB; glide along a B− plane does not. Glide of dislocations on the $(\bar{1}\bar{1}1)$ and (111) A planes (not shown) can also create APBs, but only if the corresponding Burgers vector is also coplanar with the B+ plane ($[011]$ or $[\bar{1}01]$). If the Burgers

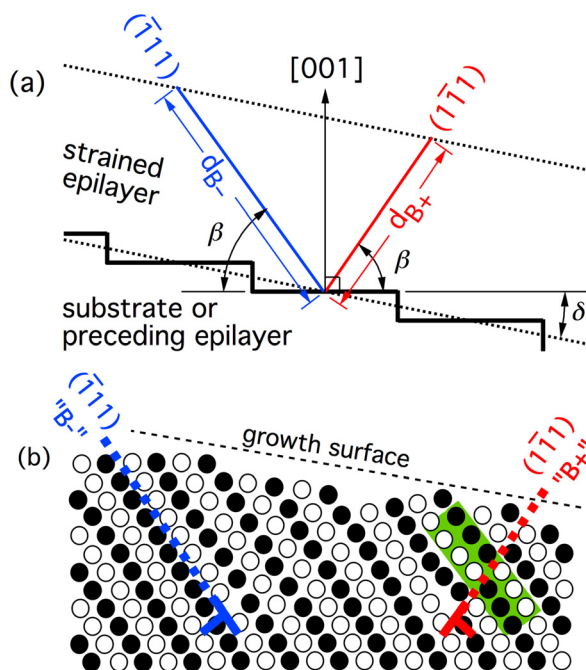


FIG. 1. (a) Sample geometry, with the size of the substrate steps exaggerated for the purposes of illustration. In the actual experiment, the epilayer thickness of $0.25\ \mu\text{m}$ is much greater than the step height. (b) Schematic diagram of the ordering pattern corresponding to the miscut direction shown in (a). Black layers are In-rich; white layers are Ga-rich. APBs can be created by glide on the B+ plane, but not the B− plane. The supercell used for calculations is a longer version of the shaded rectangle, containing two equally spaced APBs so as to be periodic, and located in bulk-like material far from both the surface and the dislocation core (Figure 2).

vector is coplanar with the B− plane ($[01\bar{1}]$ or $[\bar{1}0\bar{1}]$), no APB will result. Later in this paper, we will show how these asymmetries can cause the glide plane to switch between B− and B+, but to do this we must first compute E_{APB} .

III. ANTIPHASE BOUNDARY ENERGY (E_{APB})

To compute E_{APB} , *ab initio* total-energy calculations were performed for a supercell of fully ordered $\text{Ga}_{0.5}\text{In}_{0.5}\text{P}$, first without an APB, and then with APBs of various spacings. Total energies were calculated using the screened Heyd-Scuseria-Ernzerhof (HSE) hybrid density functional,¹⁴ as implemented in the VASP package.¹⁵ Our DFT calculations employed the projector augmented wave method¹⁶ with an energy cutoff of 270 eV for the plane wave part of the wave function. The atomic coordinates were fully relaxed. To obtain E_{APB} values for widely spaced APBs (for which the APB-APB interaction energy is negligible), the APB spacing was increased until E_{APB} reached a constant value; this occurred at an APB spacing of $\sim 40\ \text{\AA}$.

Figure 2 shows the resulting atomic structure near an APB viewed along the plane of the APB. No dislocation is shown; this is the APB structure which remains after a dislocation glides along the B+ plane. Because these calculations were performed for fully ordered material (ordering parameter $\eta = 1$), the resulting E_{APB} value is an upper limit which will be denoted $E_{\text{APB}}^{\text{max}}$. However, even under growth conditions favorable for ordering, the order parameter for $\text{Ga}_{0.5}\text{In}_{0.5}\text{P}$ is typically 0.4, and decreases as the alloy composition moves away from $x = 0.5$. Therefore, the APB energy for partially ordered material will be approximated with an η^2 scaling factor: $E_{\text{APB}} = E_{\text{APB}}^{\text{max}} \cdot \eta^2$.^{1,17}

Calculated values of $E_{\text{APB}}^{\text{max}}$ for three representative III-V alloys are shown in Table I. Negative values indicate that an APB-creating dislocation will lower the energy of the system as it glides, thereby providing a driving force for dislocation glide $\tau_{\text{APB}} = -E_{\text{APB}}$, where τ_{APB} is a force per unit dislocation line length and E_{APB} is an energy per unit area. Using special quasi-random structures^{3,18} or random alloy models, the energy released by disordering a unit volume of each alloy ($E_{\text{disordering}}$) was also calculated. It is interesting to note that $E_{\text{APB}}^{\text{max}}$ and $E_{\text{disordering}}$ are roughly proportional to each

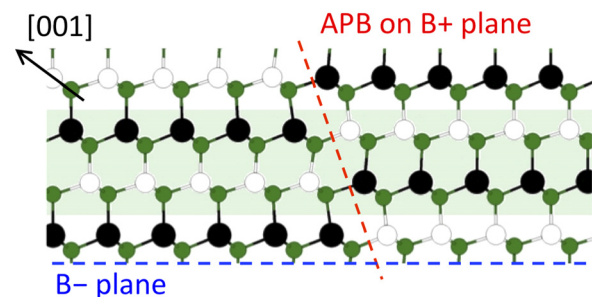


FIG. 2. Relaxed atomic structure of an APB on a B+ plane in fully ordered GaInP_2 . Distortion of the bond angles can be seen near the APB. Black atoms are In, white atoms are Ga, and green-shaded atoms are P. The (green) shaded rectangle is the central portion of the widest supercell used in our calculations. Each supercell contains two APBs so as to be periodic. This figure is rotated counter-clockwise with respect to Figure 1.

TABLE I. An ordered III-V alloy stores energy which can be released by forming an APB (via dislocation glide) or by disordering the material (via annealing). The values shown are calculated energies for these two processes, E_{APB}^{max} and $E_{disordering}$, respectively. A negative value for E_{APB}^{max} indicates that APB formation enhances dislocation glide (see text). Values for $Al_{0.5}Ga_{0.5}P$ and $Al_{0.5}Ga_{0.5}As$ were approximately zero to within the computational uncertainty.

Alloy	E_{APB}^{max} (meV/Å ²)	$E_{disordering}$ (meV/Å ³)
$Al_{0.5}In_{0.5}P$	-10.7	-0.74
$Ga_{0.5}In_{0.5}P$	-9.9	-0.70
$Ga_{0.5}In_{0.5}As$	-7.5	-0.52

other, and that the proportionality factor of ~ 14 Å is similar to the extent of the bond-angle distortions seen in Fig. 2.

IV. GLIDE-PLANE SWITCHING EXPERIMENT

A. Description

We will now show that the value of E_{APB}^{max} for $Ga_{0.5}In_{0.5}P$ can be directly linked to experimental observation via a glide-plane switching experiment² which is particularly sensitive to the value of E_{APB}^{max} . The essential idea is to compare the driving force of APB formation to competing forces generated by compressive epilayer strain.

In this experiment, partially ordered $Ga_xIn_{1-x}P$ epilayers are grown compressively strained on a (001) substrate miscut δ degrees toward $(\bar{1}11)B$ using the sample geometry shown in Figure 1. In this configuration, relief of the compressive epilayer strain favors dislocation glide on the B− plane,¹⁹ whereas APB formation favors glide on the B+ plane. Conditions are chosen such that dislocation glide is observed on the B+ plane for an initial value of η , then η for each subsequent epilayer is reduced (by reducing the Ga fraction x) until the glide switches to the B− plane at a value η_{gps} , where “gps” denotes “glide-plane switch.” The ordering parameter for lattice-matched $Ga_{0.5}In_{0.5}P$ is measured using XRD²⁰ and assumed to be proportional to the Ga fraction as it is incrementally reduced to zero in subsequent layers: $\eta(x) = \eta(0.5) \cdot 2x$ for $Ga_xIn_{1-x}P$ for $0 \leq x \leq 0.5$. Residual stress is monitored during growth using a multibeam optical stress sensor (MOSS).²¹ After an initial period of coherently strained growth, relaxation commences and holds the residual strain in the uppermost (relaxing) epilayer to a fairly constant value $\epsilon = -0.1\%$. Using these methods, experimental η_{gps} values can be extracted from XRD data (Figure 3(a)) and compared to modeled values (to be computed next). A more complete description of the sample configuration and determination of η_{gps} is provided in the caption of Figure 3.

B. Theory

To compute η_{gps} , the glide-inducing stress for each plane (τ_{B+} and τ_{B-}) must be computed and compared; at η_{gps} the difference $\Delta\tau = \tau_{B+} - \tau_{B-}$ is zero. The values of τ_{B+} and τ_{B-} are defined to be the work done per unit length of dislocation as it advances a unit distance, divided by the area swept.²² Because τ_{B+} is altered by APB formation, it is a

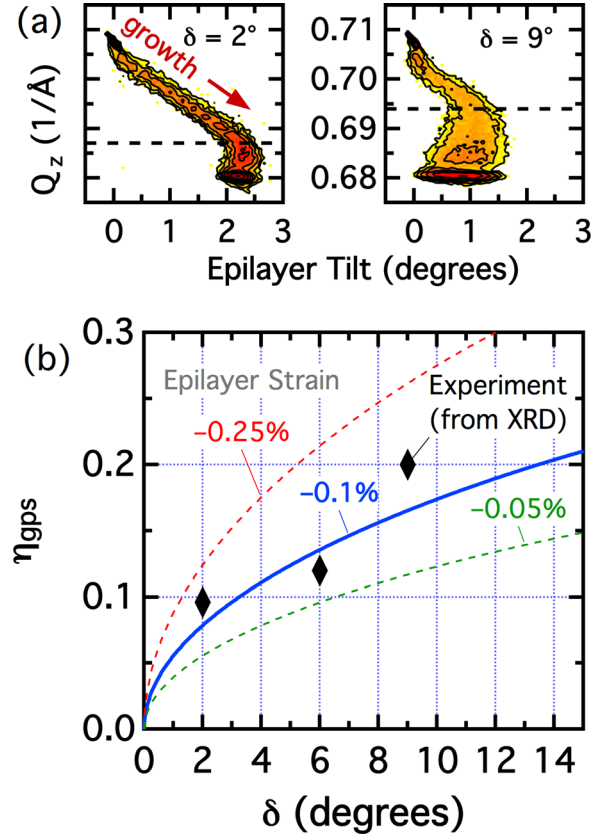


FIG. 3. (a) Experimental [004] XRD reciprocal space maps for $Ga_xIn_{1-x}P$ lattice-mismatched grades grown on $GaAs(001)$ miscut δ degrees toward $(\bar{1}11)B$. Epilayer tilt is toward $[1\bar{1}0]$ and $Q_z = 4/a_z$, where a_z is the lattice constant in the $[001]$ direction. The substrate peak is at the upper left corner of each plot, and the $Ga_xIn_{1-x}P$ grade concludes with an InP layer at the bottom of each plot. Both Q_z and η for each subsequent $Ga_xIn_{1-x}P$ layer decrease as the lattice constant increases. For all layers grown before the glide plane switch (dashed line), dislocations glide predominantly on the $(\bar{1}\bar{1}1)B+$ plane and increase the epilayer tilt. After the glide plane switch, preferential glide on the $(\bar{1}\bar{1}1)B-$ plane reduces the epilayer tilt. (b) Theoretical η_{gps} values plotted as a function of sample miscut angle δ for different residual strains ϵ with $E_{APB} = E_{APB}^{max} \cdot \eta^2$, where $E_{APB}^{max} = -9.9$ meV/Å². Experimental η_{gps} values for three different substrate miscut angles are plotted as points.

function of η ; τ_{B-} is not. The resulting equations for τ_{B+} and τ_{B-} can be obtained by dividing the configurational force on a dislocation for each glide plane (for the entire epilayer thickness h)²² by the surface-to-interface distance as measured along each glide plane (d_{B+} and d_{B-} in Figure 1):

$$\tau_{B+} = M \cdot |\epsilon| \cdot b_{misfit}^{B+} \cdot \sin(\beta + \delta) - E_{APB}^{max} \cdot \eta^2 - \tau_{line}^{B+}, \quad (1)$$

$$\tau_{B-} = M \cdot |\epsilon| \cdot b_{misfit}^{B-} \cdot \sin(\beta - \delta) - \tau_{line}^{B-}, \quad (2)$$

where the (strain-relieving) misfit components of the Burgers vector \mathbf{b} for 60° dislocations gliding on the B+ and B− planes are

$$b_{misfit}^{B+} = \frac{\sqrt{3}}{2\sqrt{2}} \cdot a_0 \cdot \cos(\beta + \delta), \quad (3)$$

$$b_{misfit}^{B-} = \frac{\sqrt{3}}{2\sqrt{2}} \cdot a_0 \cdot \cos(\beta - \delta), \quad (4)$$

and a_0 is the lattice constant, M is the biaxial modulus for the epilayer, β is the angle between (001) and each B plane (B+ and B-), and τ_{line} accounts for the energy of the additional dislocation line length created by dislocation glide. Because τ_{line}^{B+} and τ_{line}^{B-} will be small and similar for $h \gg |\mathbf{b}|$, they are neglected when solving for η_{gps} by setting $\Delta\tau = \tau_{B+} - \tau_{B-}$ to zero:

$$\eta_{gps} = \sqrt{\frac{M \cdot |\epsilon|}{E_{APB}^{max}} \cdot \frac{\sqrt{3}}{2\sqrt{2}} \cdot a_0 \cdot \cos(2\beta) \cdot \sin(2\delta)}. \quad (5)$$

It should be noted that Eq. (5) can also be applied to dislocation nucleation. The derivation is analogous to that shown above, but for nucleation the τ_{line} terms account for the dislocation half-loop and surface step formed during nucleation. By symmetry, these terms are similar on the two planes ($\tau_{line}^{B+} \approx \tau_{line}^{B-}$); Eq. (5) is obtained if their difference is neglected.

Before discussing results for a specific set of parameters, it is instructive to consider the dependence of η_{gps} on β for $E_{APB}^{max} < 0$, keeping in mind that the actual value of β is a constant determined by the crystal structure of the epilayer. First of all, $\eta_{gps} = 0$ for $\beta = 45^\circ$. This is because the resolved shear stress (Schmid factor²³) is symmetric with angle about a maximum at 45° ; in the absence of ordering (i.e., for $\eta = 0$), the resolved shear stress would be equal on the B+ and B- planes for any given value of δ if $\beta = 45^\circ$. A second limiting case is $\beta < 45^\circ$, for which glide on the B+ plane is preferred. Because ordering can only enhance this preference, there is no real value of η which can cause $\Delta\tau$ to be zero and thereby cause dislocation glide to switch to the B- plane. Finally, for $\beta > 45^\circ$ (as it is for a zincblende lattice), glide on the B- plane is preferred for $\eta = 0$, and switches to the B+ plane for $\eta > \eta_{gps}$.

C. Results

The η_{gps} values plotted in Figure 3(b) were calculated using parameters corresponding to our experimental configuration: $a_0 = 5.653 \text{ \AA}$ for $\text{Ga}_x\text{In}_{1-x}\text{P}$ lattice-matched to GaAs, $M = 0.759 \text{ eV/\AA}^3$ for $\text{Ga}_{0.5}\text{In}_{0.5}\text{P}$, interpolated linearly between GaP and InP values,²⁴ and $\beta = \cos^{-1}(1/\sqrt{3}) = 54.74^\circ$. For simplicity, small changes from these values as a function of composition x are neglected. Lines are plotted as a function of δ for three different ϵ values; glide will be on the B+ plane above each line, and on the B- plane below each line. As either δ or ϵ is increased, a larger value of η is needed to switch glide from the B- plane to the B+ plane. To provide data for comparison, a set of samples was grown with three different miscut angles δ .

In comparing the data to the theory, it is important to note that the theory has been limited to only the relaxation processes discussed above, and the assumptions for extracting experimental parameters have been kept as simple as possible. Despite these simplifications, the agreement is quite good and indicates that the basic model discussed above captures the essential physics. Most significantly, the initial B+ glide indicates that E_{APB} is negative. If E_{APB} were positive, then B- glide would always be preferred, and η_{gps}

from Eq. (5) would be imaginary. It is also significant that the theoretical η_{gps} values plotted in Fig. 3(b) are less than the maximum allowed value (1 in general, ~ 0.4 for $\text{Ga}_{0.5}\text{In}_{0.5}\text{P}$). This indicates that the theoretical E_{APB} value is large enough to cause the observed glide-plane switch; if it were not, then η_{gps} from Eq. (5) would exceed the allowed range for η . Finally, the theoretical E_{APB}^{max} value produces an η_{gps} curve for $\epsilon = -0.1\%$ which is near the experimental values for $\epsilon \approx -0.1\%$, and exhibits a similar increase with δ .

V. IMPLICATIONS

The agreement between theory and experiment illustrates two key points. First, it provides an experimental confirmation of the theoretical E_{APB}^{max} value. Even more significantly, it illustrates how a negative E_{APB}^{max} value can alter relaxation processes during lattice-mismatched epitaxy. The remainder of this paper will focus on possible consequences.

One consequence is already established experimentally: APB-related glide-plane switching can cause the threading dislocation density in an epitaxial film to dramatically increase.² Because glide-plane switching balances the driving force of APB formation against competing forces induced by epilayer strain, it is particularly sensitive to the value of E_{APB} and was therefore chosen as the test system for this paper. However, E_{APB} alters every equation describing dislocation motion, and can therefore be expected to affect a wide range of stress-relaxation processes.

The APB energy should alter the critical thickness for initial relaxation, for example. The extra glide force provided by E_{APB} may also increase the average glide length, thereby reducing both the residual strain and threading dislocation density during lattice-mismatched growth. Nucleation of new dislocations at the surface may also be enhanced. The passage of many APB-generating dislocations through a material will generate a network or array of stable APBs which can alter some material properties,⁹ and may also affect the motion of subsequent dislocations. Additional consequences of metastable ordering on stress relaxation will likely be discovered and may extend beyond III-V alloys to other material systems.

Finally, to fully appreciate the influence of the growth surface on all of the processes discussed in this paper, the interrelationship between the surface and APBs should be considered. Cross-sectional TEM shows that pairs of APBs tend to attract and annihilate despite their stability in the bulk, reducing the APB density as growth proceeds.⁸ This suggests that APBs terminate at high-energy surface structures (undimerized P atoms, for example), which provide an energetic driving force for APB annihilation. In other words, surface energetics may be responsible not just for the creation of metastable ordering, but also for reducing the APB density to produce large APB-free ordered domains, thereby creating ideal conditions for APB-enhanced dislocation glide.

VI. SUMMARY

In summary, we show that metastable sublattice ordering of III-V alloys can dramatically alter stress relaxation

mechanisms. In the example considered here, sublattice ordering causes the glide of strain-relieving dislocations to switch to a different glide plane. Theoretical modeling links this glide plane switch to the stability of dislocation-created APBs in the ordering pattern. The stability of an APB is characterized by a maximum value for fully ordered material, E_{APB}^{max} , which can be used to modify all equations governing dislocation motion. The results presented here for $Ga_xIn_{1-x}P$ can readily be extended to other ordered III-V alloys. This should provide a better theoretical understanding of relaxation in ordered III-V alloys, which in turn should lead to an improvement in the quality of lattice-mismatched materials and devices grown using these alloys.

ACKNOWLEDGMENTS

This work was supported by the U.S. Department of Energy under Contract No. DE-AC36-08-GO28308 with the National Renewable Energy Laboratory. The authors would also like to acknowledge Waldo Olavarría for the growth of the samples used in this study.

- ¹A. Mascarenhas, *Spontaneous Ordering in Semiconductor Alloys* (Plenum Publishers, New York, 2002).
- ²R. M. France, W. E. McMahon, A. G. Norman, J. F. Geisz, and M. J. Romero, *J. Appl. Phys.* **112**(2), 023520 (2012).
- ³A. Zunger, S. H. Wei, L. G. Ferreira, and J. E. Bernard, *Phys. Rev. Lett.* **65**(3), 353 (1990).
- ⁴J. E. Bernard, R. G. Dandrea, L. G. Ferreira, S. Froyen, S. H. Wei, and A. Zunger, *Appl. Phys. Lett.* **56**(8), 731 (1990).
- ⁵J. S. Koehler and F. Seitz, *J. Appl. Mech.* **14**, A-217 (1947).
- ⁶M. J. Marcinkowski, R. M. Fisher, and N. Brown, *J. Appl. Phys.* **31**(7), 1303 (1960).

- ⁷C. S. Baxter, W. M. Stobbs, and C. J. Gibbings, *Philos. Mag. Lett.* **67**(1), 59 (1993).
- ⁸E. Spiecker, M. Seibt, W. Schröter, R. Winterhoff, and F. Scholz, *Appl. Surf. Sci.* **188**(1–2), 61 (2002); E. Spiecker, *Philos. Mag.* **86**(29–31), 4941 (2006).
- ⁹T. Mattila, S.-H. Wei, and A. Zunger, *Phys. Rev. Lett.* **83**(10), 2010 (1999).
- ¹⁰D. J. Friedman, *Curr. Opin. Solid State Mater. Sci.* **14**(6), 131 (2010).
- ¹¹J. E. Ayers, S. K. Ghandhi, and L. J. Schowalter, *J. Cryst. Growth* **113**(3–4), 430 (1991); P. M. Mooney, F. K. LeGoues, J. Tersoff, and J. O. Chu, *J. Appl. Phys.* **75**(8), 3968 (1994).
- ¹²S. B. Zhang, S. Froyen, and A. Zunger, *Appl. Phys. Lett.* **67**(21), 3141 (1995).
- ¹³P. Gavrilovic, F. P. Dabkowski, K. Meehan, J. E. Williams, W. Stutius, K. C. Hsieh, N. Holonyak, Jr., M. A. Shahid, and S. Mahajan, *J. Cryst. Growth* **93**(1–4), 426 (1988).
- ¹⁴J. Heyd, G. E. Scuseria, and M. Ernzerhof, *J. Chem. Phys.* **118**(18), 8207 (2003).
- ¹⁵G. Kresse and J. Furthmüller, *Phys. Rev. B* **54**(16), 11169 (1996).
- ¹⁶P. E. Blöchl, *Phys. Rev. B* **50**(24), 17953 (1994); G. Kresse and D. Joubert, *ibid.* **59**(3), 1758 (1999).
- ¹⁷D. B. Laks, S.-H. Wei, and A. Zunger, *Phys. Rev. Lett.* **69**(26), 3766 (1992).
- ¹⁸S. H. Wei, L. G. Ferreira, J. E. Bernard, and A. Zunger, *Phys. Rev. B* **42**(15), 9622 (1990).
- ¹⁹F. Riesz, *J. Appl. Phys.* **79**(8), 4111 (1996); R. S. Goldman, K. L. Kavanagh, H. H. Wieder, S. N. Ehrlich, and R. M. Feenstra, *ibid.* **83**(10), 5137 (1998).
- ²⁰R. L. Forrest, T. D. Golding, S. C. Moss, Y. Zhang, J. F. Geisz, J. M. Olson, A. Mascarenhas, P. Ernst, and C. Geng, *Phys. Rev. B* **58**(23), 15355 (1998).
- ²¹J. F. Geisz, A. X. Levander, A. G. Norman, K. M. Jones, and M. J. Romero, *J. Cryst. Growth* **310**(7–9), 2339 (2008).
- ²²L. B. Freund and S. Suresh, *Thin Film Materials: Stress, Defect Formation and Surface Evolution* (Cambridge University Press, New York, 2003).
- ²³J. P. Hirth and J. Lothe, *Theory of Dislocations* (Krieger Publishing Company, Malabar, FL, 1992).
- ²⁴S. Adachi, *Properties of Semiconductor Alloys: Group-IV, III-V and II-VI Semiconductors* (John Wiley and Sons Ltd., Chichester, West Sussex, UK, 2009).